Available online at www.sciencedirect.com

ScienceDirect

Chinese Journal of Natural Medicines 2019, **17**(10): 0756–0767

Chinese Journal of Natural Medicines

Pilose antler aqueous extract promotes the proliferation and osteogenic differentiation of bone marrow mesenchymal stem cells by stimulating the BMP-2/Smad1, 5/Runx2 signaling pathway

REN Cong[1], GONG Wei[2], LI Feng[1*], XIE Ming[1*]

[1] *School of Pharmacy, Liaoning University of Traditional Chinese Medicine, Dalian 116600, China;*
[2] *Affiliated Hospital of Liaoning University of Traditional Chinese Medicine, Shenyang 110032, China*

Available online 20 Oct., 2019

[ABSTRACT] Peptides from Pilose antler aqueous extract (PAAE) have been shown to stimulate the proliferation and differentiation of bone marrow mesenchymal stem cells (BMSCs). However, the underlying molecular mechanisms are not well understood. Here, PAAE was isolated and purified to explore the molecular mechanisms underlying PAAE's effects on BMSCs as well as its osteoprotective effects in ovariectomized rats. Our results showed that PAAE promoted proliferation and differentiation of BMSCs to become osteoblasts by enhancing ALP activity and increasing extracellular matrix mineralization. The trabecular microarchitecture of ovariectomized rats was also found to be protected by PAAE. Quantitative reverse transcription-polymerase chain reaction (Quantitative RT-PCR) results suggest that PAAE also increased the expression of osteogenic markers including, alkaline phosphatase (ALP), runt-related transcription factor 2 (Runx2), osteocalcin (OCN), bone morphogenetic protein-2 (BMP-2), and collagen I (COL-I). Immunoblotting results indicated that PAAE upregulated the levels of BMP-2 and Runx2 and was associated with Smad1/5 phosphorylation. PAAE A at the concentration of 200 $\mu g \cdot mL^{-1}$ showed the strongest effect on proliferation and osteogenic differentiation of BMSCs after 48 h. Using matrix-assisted laser desorption/ionization time of flight mass spectrometry (MALDI-TOF MS), we identified the molecular weight of PAAE A and found that it is less than 3000 Da and showed several significant peaks. In conclusion, PAAE activates the BMP-2/Smad1, 5/Runx2 pathway to induce osteoblastic differentiation and mineralization in BMSCs and can inhibit OVX-induced bone loss. These mechanisms are likely responsible for its therapeutic effect on postmenopausal osteoporosis.

[KEY WORDS] Pilose antler; Postmenopausal osteoporosis; Bone marrow mesenchymal stem cells; BMP-2/Smad1, 5/Runx2 signaling pathway

[CLC Number] R965 **[Document code]** A **[Article ID]** 2095-6975(2019)10-0756-12

Introduction

Postmenopausal osteoporosis (Pmo) is a major health problem throughout the world [1-2]. This disease increases bone fragility and the risk of fractures and impairs the healing of bone defects in older women.

At present, inhibitors of bone resorption, including calcitonin, bisphosphonates, and estrogens, are extensively used to treat osteoporosis [3]. These drugs modulate bone density by inhibiting osteolysis, however, long-term administration of these drugs may harm human health. The American Disease Prevention Task Force recommends that estrogen be used for the prevention of osteoporosis, preferably for less than three years. The Menopause Group of the Obstetrics and Gynecology Branch of the Chinese Medical Association concurs and recommends that the use of estrogen should not exceed two years. The main adverse effects of estrogen arepostmenopausal vaginal bleeding and increased incidence of breast cancer, endometrial cancer, deep vein thrombosis, and pulmonary embolism. Due to the severity of these side effects, many patients choose an alternative or complementary medicine—such as traditional Chinese medicine—to prevent and treat postmenopausal osteoporosis.

Pilose antler (*Cervus elaphus* Linnaeus; *cervi cornu pantotrichum* in Latin) is known as "lu rong" in Chinese, "nokyong" in Korean, and "tokujo" in Japanese, is exten-

[Received on] 08-July-2019
[Research funding] The work was supported by the National Natural Science Foundation of China (No. 81473314).
[*Corresponding authors] E-mails: zhanglijiayi@163.com (LI Feng); x6m6@163.com (XIE Ming)
These authors have no conflict of interest to declare.

sively used as a herbal medicinal supplement throughout East Asia. Moreover, the medicinal properties make pilose antler a useful biomedical model for the exploration of regenerative processes in mammalian tissues and organs. Pilose antler is used in traditional Chinese medicine to improve kidney function, stimulate blood circulation, treat neurasthenia, strengthen muscles and bones, and prolong life [4]. Previous studies have shown that pilose antler herbs can stimulate the proliferation and differentiation of osteoblasts and confer both preventive and therapeutic effects for osteoporosis in ovariectomized rats [5-6].

Pilose antler contains many organic molecules, including phospholipids, glycolipids, gum lipids, hormones, fatty acids, amino acids, proteins, as well as minerals such as calcium, phosphorus, magnesium, sodium, and others. Of these constituents, amino acids are the most prevalent, accounting for more than 50% of all constituents [7].

However, whether these substances are responsible for the effectiveness of pilose antler in preventing and treating osteoporosis remains unknown.

In this study, we hypothesize that the most abundant constituents found in pilose antler extracts (i.e. amino acids, peptides, and/or proteins) are the pharmacologically active components in pilose anther herbal medicines; thus, we studied the effects of various pilose antler aqueous extracts on BMSCs and ovariectomized (OVX)-induced rats. By evaluating the pharmacological efficacy of these extracts in promoting bone differentiation and formation, we aimed to determine how, to some degree, the active ingredient in pilose antler extracts (hereafter, "substance A") can prevent and/or treat osteoporosis. Finally, we also identified and characterized substance A and explored the mechanism responsible for its action on the physiological responses of postmenopausal osteoporosis.

Materials and Methods

Reagents, antibodies, and animals

Progynova (No. 287A) was purchased from Bayer (Leverkusen, Germany); the *XianLingGuBao* tablets (XLGB (No. 160709)) were purchased from Guizhou Tongjitang Pharmaceutical Co., Ltd. (Guizhou, China); the bicinchoninic acid (BCA) kits for protein concentration determination were purchased from Beyotime (Shenyang, China). Primary anti- bodies raised against phosphorylated-Smad1 (Ser463/465)/ Smad5 (Ser463/465) and unphosphorylated Smad1/5 were purchased from Cell Signaling Technology (Danvers, USA). Other primary antibodies used for Western blotting were obtained from AMEKO (Shanghai, China).

Female Sprague Dawley (SD) rats (250 ± 20 g, 12 weeks old) were purchased from Liaoning Changsheng Biotechnology Co., Ltd. (Benxi, China; license number C-LN2017040722). SD rat BMSCs (batch No. 090905B01) were purchased from Cyagen (Santa Clara, USA). Rats were fed and housed at the Laboratory Animal Facility at Liaoning University of Traditional Chinese Medicine (Shenyang, China). Housing conditions, including temperature (22–24 °C), humidity (50%–60%) and light/dark cycle (12 h/12 h), were tightly controlled. Rats were given adequate water and food supply. Prior to all experiments, rats were habituated for at least seven days. Animal experiments were carried out following the guidelines for the Care and Use of Laboratory Animals of the National Institute of Health. This study was approved and supervised by the Animal Care and Use Committee of Liaoning University of Traditional Chinese Medicine.

Preparation of pilose antler aqueous extract

The optimal method for extracting pilose anther aqueous extract (PAAE) was as follows: the granularity of pilose antler samples was 80–100 mesh, the ratio of sample material to water was 1 : 12 (*W*/*V*), and extraction was performed three times (20 minutes per extraction). The protein content of pilose antler aqueous extracts was determined using Bradford assays, with a mean protein concentration of 37.02 $mg \cdot g^{-1}$. The molecular weight distribution of the proteins within the PAAE samples was determined by SDS-PAGE and high- performance gel chromatography. PAAE samples were separated and purified by multi-membrane separation. Separated proteins sourced from PAAE samples were separated into five segments by different (i.e. 100, 50, 10, 5, and 3 kDa) ultrafiltration membrane and a 0.2 kDa nanofiltration membrane. Molecular weight of the five classes of protein components found in PAAE samples was as follows: PAAE A (200–3000 Da), PAAE B (3000–5000 Da), PAAE C (5000–10 000 Da), PAAE D (10 000–50 000 Da), and PAAE E (> 50 000 Da). Finally, we also dried all samples (i.e. PAAEs A–E) using concentration-ultrafiltration-concentration-freeze-drying to obtain freeze-dried powders for each protein class.

Cell culture

The BMSCs were cultured in dulbecco's modified eagle medium (DMEM) medium supplemented with 10% fetal bovine serum and antibiotics (1% penicillin and 1% streptomycin) at 37 °C and 5% CO_2. Cell culture media was changed twice a week.

Cell proliferation

The proliferation of BMSCs was evaluated by 3-(4, 5-dimethyl-2-thiazolyl)-2, 5-diphenyl-2-H-tetrazolium, bromide Thiazolyl Blue Tetrazolium Bromide (MTT) assays. Briefly, BMSCs (1×10^4) at passage two were plated into 96-well plates and incubated in a complete medium for 24, 48, or 72 h before treated with 50, 100, or 200 $\mu g \cdot mL^{-1}$ PAAE (A, B, C, D, or E). The medium was refreshed every three days. After 48 h, 20 μL of MTT solution (5 $g \cdot L^{-1}$, *W*/*V*) was added to the medium after four hours of incubation, the cell culture medium in each well was removed and 150 μL Dimethyl sulfoxide (DMSO) was added. Next, the optical density at 570 nm was recorded for all samples.

Cell osteogenic differentiation

BMSCs (1×10^4) were seeded into the 24-well cell culture plates and cultured in a complete medium for 48 h before treated with 200 μg·mL^{-1} PAAE. The medium was changed every three days afterward. Fetal bovine serum was used as a blank control, and the induction solution (MEM containing 10% FBS, 1% penicillin, 1% streptomycin, 10^{-8} mol·L^{-1} dexamethasone, 10 mmol·L^{-1} β-glycerophosphate, and 50 μg·mL^{-1} ascorbic acid) was used for the positive control group. After inducing the culture for 6, 9, and 12 d, the respective activities of ALP, BMP-2, and BGP were determined using the enzyme-linked immunosorbent assay (ELISA) following the manufacturer's protocol.

RNA isolation, reverse transcription, and polymerase chain reaction (PCR)

After culturing the BMSCs (1×10^5) for 48 h, total RNA was isolated using PrimeScript® RT with gDNA Eraser. Next, 0.5 μg of the total RNA was reverse transcribed into cDNA using the reverse transcription kits (PrimeScript® RT reagent Kit with gDNA Eraser). RT-qPCR was performed on a Stratagene Mx3000p Fluorescence quantification PCR instrument using SYBR® Premix Ex Taq™ ((TliRNaseH Plus) and a ROXplus reagent Kit. The PCR program was: 42 °C for 2 min, 95 °C for 10 min, followed by 40 cycles of 95 °C for 5 sec, 60 °C for 1 min, and 72 °C for 30 sec. Fluorescent signals were detected once every time the temperature increased from 55 to 95 °C. All reactions were performed in triplicate. The Stratagene Mx3000p software was used to analyze the PCR data, and the β-actin gene was used as an internal control. The sequences of all primers are shown in Table 1.

Western blotting analysis

The BMSCs (2.5×10^4) were passaged for three generations and then cultured in 1 mL medium in the six-well cell culture plates. The medium was changed twice per week. Cells were pelleted and cell lysis was carried out using a lysisbuffer. After a five min denaturation at 98 °C, cell lysates were separated by sodium dodecyl sulphate-polyacrylamide gel electrophoresis (SDS-PAGE) and were electro-transferred (30 V) to a nitrocellulose membrane. The membrane was incubated with the primary antibodies (rabbit anti-rat BMP-2 [1 : 3000], Smad1/5 [1 : 3000] and Runx2 [1 : 3000]) at 4 °C overnight and were then probed with a goat anti-rabbit IgG secondary antibody (1 : 5000). The level of ACTB protein was analyzed as a positive control. Protein bands were visualized following the instructions of the BCA-200 Protein Quantification Kit and the densitometry analysis was performed using the Image J2X software.

Table 1 Primer sequences

Gene Name	GeneBank Number		Primer sequence (5'-3')	Product length (bp)
Bmp-2	NM_017178	F	5'-CTGCGGTCTCCTAAAGGTCG-3'	180
		R	5'-ACTCAAACTCGCTGAGGACG-3'	
Smad1	NM_013130	F	5'-GCAGTTGCTTACGAGGAACC-3'	223
		R	5'-GGTGGACTCCTTTCCCGATG-3'	
Smad5	NM_021692	F	5'-AGCAGAGATGTTCAGCCTGT-3'	213
		R	5'-GCCTGGTGTTCTCGATGGTT-3'	
Runx2	NM_001278483	F	5'-GCCTTCAAGGTTGTAGCCCT-3'	178
		R	5'-TGAAACTCTTGCCTCGTCCG-3'	
β-actin	NM_031144	F	5'-CGCGAGTACAACCTTCTTGC-3'	70
		R	5'-CGTCATCCATGGCGAACTGG-3'	

Determination of calcified matrix

Mineralization of the BMSCs was evaluated using the Alizarin red S staining method, in which calcium salts are selectively stained dark red by Alizarin red. Briefly, PAAE A (determined to have the best effect by the cell proliferation and osteogenic differentiation assays) was added to 2×10^5 BMSCs to a final concentration of 200 μg·mL^{-1} and the mixture was incubated for 21 d. Next, the cells were stained with 40 mmol·L^{-1} Alizarin red S (pH 4.2) and calcified extracellular matrices were detected and photographed using a light microscope (Nikon, Japan). To quantify the calcified extracellular matrices, cetylpyridinium chloride was added to the Alizarin red-stained cells to a final concentration of 100 mmol·L^{-1} and the mixture was incubated for 1 h. After incubation, the optical density of all samples was determined at 570 nm using a plate reader.

Establishment of an ovariectomy-induced rat osteoporosis model

Rats were randomly divided into six groups with 10 rats in each group. Five groups of rats were ovariectomized (OVX)—these included the OVX control group, the OVX + high dosage PAAE-treated group, the OVX + low dosage PAAE-treated group, the Western Medicine positive control group (Progynova, 0.025 mg·mL^{-1}), and the traditional Chinese medicine positive control group (XLGB, 0.045 g·mL^{-1}). The remaining one groups was the normal control group.

The rats were anesthetized with 10% chloral hydrate (3.5 mL/kg body weight via intraperitoneal injection) and a bilateral ovariectomy was carried out. Seven days after the surgery, PAAE was administered to the OVX rats (*via* daily

intragastric administration of PAAE at 0.14 g·kg^{-1} and 1.26 g/kg body weight for in the low- and high-dosage PAAE groups, respectively), and the administration was continued for 12 weeks. Rats in the normal control group were not ovariectomized and were treated orally with water for 12 weeks. Rats were executed by the abdominal aorta for blood collection. The femurs were then obtained and immediately subjected to 4% paraformaldehyde fixation for future use. The levels of ALP, OCN, BMP-2, estrogen (E2), tartrate-resistant acid phosphatase (TRAP), and peroxisome proliferator-activated receptor γ-2 (PPARγ-2) in the serum were determined using the rat ELISA kit. Levels of bone alkaline phosphatase (BALP), BMP-2, Smad1, Smad5, Runx2 and transforming growth factor-β1 (TGF-β1) levels in the bone tissues were also analyzed by ELISA.

Measurement of the microstructural parameters of femoral trabecula

Bone mineral density (BMD), bone mass/tissue volume (BV/TV), bone surface/tissue volume (BS/TV), space among the trabecular bones (Tb.Sp) and the number of trabeculae (Tb.N) were the microstructural indicators used here for further analyses. Each of the above parameter was directly determined using the stereoscopic images of trabeculae. We used a cone beam micro-computed tomography (CT) system to determine the microstructural parameters of the trabeculae of the left femur of each rat. The basic parameters of the system were as follows: X-ray voltage: 30 kV, current: 200 μA, rotation angle: 0.5°.

Hematoxylin and eosin stain (HE)

Rat femur tissue block removal was carried out in the premade fixative (10% formalin, Bouin's fixative, etc.) that was designed to denature tissues and cells while maintaining the original morphological structure. After fixing in 4% paraformaldehyde overnight at 4 °C, the tissues were decalcified using 10% EDTA. After decalcification, the samples were paraffin-embedded, sectioned, and subjected to hematoxylin and eosin (H&E) staining. H&E stained sections were examined under a light microscope.

RNA isolation from bone tissue

The rat femurs were weighed, normal saline was added, and this mixture was ground in an ice water bath to form a 10% bone tissue homogenate. After centrifugation, we extracted the supernatant. RNA was isolated as per the method described above in section 2.5.

Protein extraction from bone tissues

Bone tissue was extracted as specified above (2.11) and protein was isolated from the tissue as per the method described above in section 2.6.

Identification and characterization of PAAE A

The absorbance and the characteristic absorption peak of PAAE A were measured using ultraviolet (UV) and infrared spectrophotometers (IR). The microstructure of PAAE A was determined with an atomic force microscopy (AFM).

AFM sample preparation and observation

PAAE (0.5 mg) were weighed and distilled water was added to yield a 50 μg·mL^{-1} solution. This solution was then stirred for 4 h using a magnetic stirrer. The dissolved solution was then diluted to 1 μg·mL^{-1} with distilled water and 5 μL of the diluted solution was dripped on the surface of the newly stripped mica. The mica was let dry overnight and atomic force microscope observations were performed.

Conditions used for AFM tests

AFM tests were performed using the following parameters: Scan Size: 5 μm; Scan Rate: 0.999 Hz; Samples/Line: 256; Lines: 256; Line Direction: Retrace; Data Type: Height Sensor; Scan Line: Main; Aspect Ratio: 1.00; Capture Direction: Up; Amplitude Setpoint: 641.24 mV; and Drive Amplitude: 1310.43 mV.

Conditions used for MALDI-TOF MS

Samples were collected, air dried and dissolved in 5% trifluoroacetic acid (TFA) dissolved in 100% acetonitrile (ACN). Samples at the concentration of 1 μg·μL^{-1} were added into equal volumes of the matrix solution (α-cyano-4-hydroxycinnamic acid (CHCA) dissolved in 100% ACN containing 5% TFA to a final concentration of 10 mg·mL^{-1}). This mixture was then spotted onto an MTP 384 ground steel target plate (Bruker Daltonics, Billerica, USA) before it was left to dry at room temperature. Twenty replicates were prepared for each sample. Determined by the positive ion spectrum. Corrected with cytochrome c and trypsin inhibitor.

Results

Effect of PAAE on BMSC proliferation

We used the MTT method to examine the effect of PAAEs A–E (at concentrations of 50, 100, and 200 μg·mL^{-1} on the proliferation of BMSCs. Our results showed that PAAE increased cell proliferation in a dose-dependent manner. We concluded that PAAE has the most significant effect on promoting cell proliferation at a concentration of 200 μg·mL^{-1}. Moreover, among all the PAAE treatments examined, PAAE A exerted the strongest effect on BMSC proliferation (Fig. 1).

Effect of PAAE on Bmp-2, Smad1, Smad5, and Runx2 mRNA and protein expression in BMSCs

The transcript levels of the osteogenic markers *ALP*, *Runx2* and *BMP-2* in BMSCs were determined by qRT-PCR analysis after incubation for 48 h in 200 μg·mL^{-1} PAAEs (A–E). We found that the transcript levels of the osteogenic markers in BMSCs were significantly up-regulated by PAAEs (A–E) treatment. Overall, the effect of PAAE A on the up-regulation of Bmp-2/smad1/5—as well as on the Runx2 signaling pathway—was more significant than the effects of PAAEs B–E.(Figs. 3A–3D).

Effect of PAAE on BMSC osteogenic differentiation

As a key component of non-collagenous bone matrices, the main function of BGP is to maintain a normal bone mineralization rate and promote normal calcification during bone tissue mineral deposition. BMP-2 and ALP are specific

indicators of osteoblasts. Therefore, by measuring changes in the activity of ALP, BMP-2, and BGP, we indirectly assessed differentiation. Our results show that BMSCs have a tendency to promote bone differentiation, which indicates that PAAEs (A–E) can promote osteogenic differentiation. The activities of BGP and BMP-2 showed significant increases over time, while the ALP activity decreased and then increased. PAAE A was found to significantly increase the activities of ALP, BGP, and BMP-2 to a greater degree than PAAEs B–E. (Fig. 2).

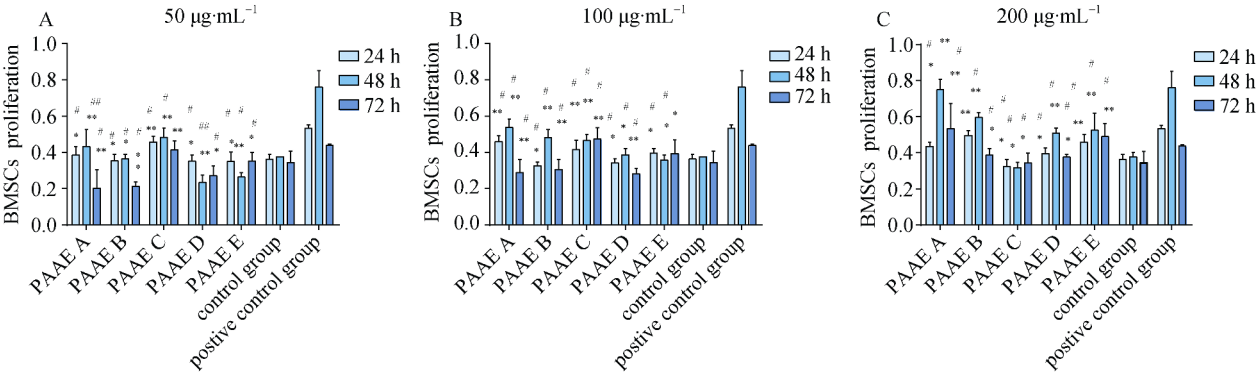

Fig. 1 Effect of the pilose antler aqueous extract (PAAE) on BMSC proliferation. Different concentrations of PAAEs (A–E) were added to the BMSCs and incubated for 24, 48, and 72 h. Viability of the BMSCs was determined by the MTT analysis. PAAEs (A–E) supplementation was found to stimulate BMSC proliferation. Data are presented as mean ± SD from three independent tests. $^{*}P < 0.05$, $^{**}P < 0.01$ *vs* control group; $^{\#}P < 0.05$, $^{\#\#}P < 0.01$ *vs* positive group

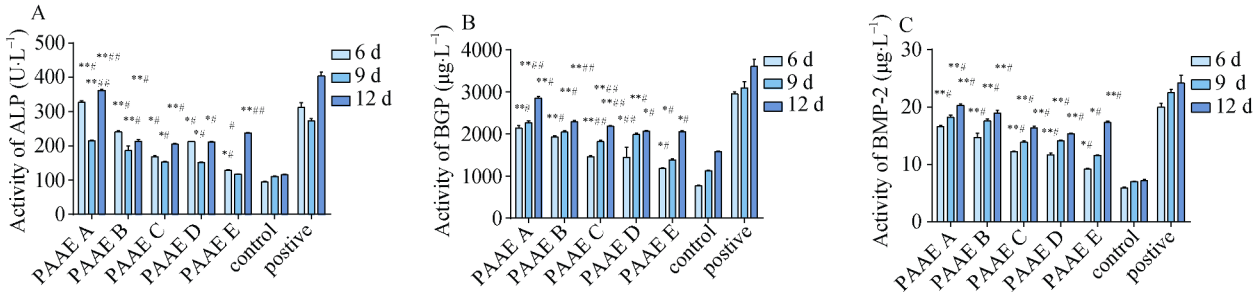

Fig. 2 The effect of pilose antler aqueous extract (PAAE) on BMSC osteogenic differentiation. Cells were treated with a 200 μg·mL^{-1} PAAEs (A–E) solution and were induced to differentiate towards osteoblasts for 6, 9 or 12 d. Activities of ALP, BMP-2, and BGP were determined by ELISA. Administration of PAAEs was found to increase the activity of ALP, BMP-2, and BGP. Data presented show the mean ± SD from three independent tests. $^{*}P < 0.05$, $^{**}P < 0.01$ *vs* control group; $^{\#}P < 0.05$, $^{\#\#}P < 0.01$ *vs* positive group

We found that PAAE promoted osteoblastic differentiation *via* BMP-2 signaling, which was known to be mediated by the downstream transcription factors Smad and Runx2. We used Western blot analysis to determine whether PAAE treatment activated BMP-2 signaling and whether PAAE affected the levels of key proteins in the BMP-2 signaling pathway (which was mediated by the BMP-2, Runx2, Smad1, and Smad5 proteins) in BMSCs. Our results indicated that the PAAEs-treated BMSCs had higher levels of these proteins than the untreated cells (Fig. 3E). The trends of the changes in protein and transcript levels are consistent. These results indicate that PAAEs treatment induced BMSCs to differentiate toward osteoblasts *via* BMP-2 signaling.

PAAE enhances ALP activity of BMSCs

ALP is an enzyme that is important for the early stages of osteogenic differentiation. We assessed the effect of PAAEs on ALP activity at various time intervals (24, 48, and 72 h). We observed no significant increase in the activity of ALP after treatment with PAAEs for 24 h. Forty-eight hours after PAAE was added, we found increased ALP activity. However, ALP activity was significantly decreased after 72 h of PAAEs treatment (Fig. 4B).

PAAE attenuates bone loss caused by ovariectomy

To investigate the effects of PAAE on osteoporosis in OVX rats, a cone beam micro-computed tomography (CT) system was used to measure the microstructural parameters of femur trabeculae. Our micro-CT results suggested that ovariectomy resulted in severe bone loss at distal femurs in rats; we observed significant decreases in BV/TV, BS/TV, and Tb.N, while Tb.Sp increased significantly. Moreover, BMD was significantly increased in response to PAAE treatment in the OVX rats. (Fig. 5A).

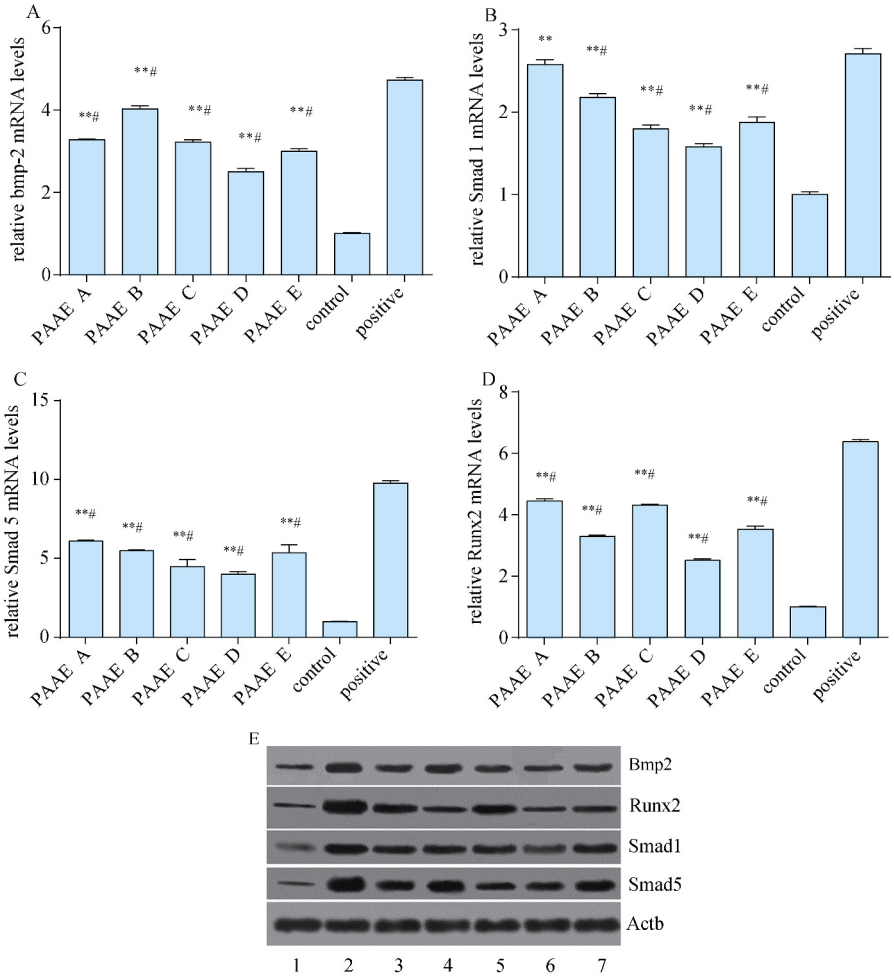

Fig. 3 Pilose antler aqueous extract (PAAE) induced BMSCs to differentiate towards osteoblasts by activating BMP-2 signaling. (A–D) BMSCs were incubated with 200 μg·mL^{-1} PAAEs for 48 h. The transcript levels of osteogenic markers were determined by qRT-PCR and the relative expression of each gene was calculated using the Piko Real Software. $^{*}P < 0.05$, $^{**}P < 0.01$ *vs* control group; $^{\#}P < 0.05$ *vs* positive group. (E) Protein levels of BMP-2, Runx2, Smad1, and Smad5 in BMSCs after PAAEs treatment. These blotting results were quantified by a densitometric assay. The electrophoretic bands labeled 1–7 represent the control group, the positive group, the PAAE A group, the PAAE B group, the PAAE C group, the PAAE D group, and the PAAE E group, respectively. Data are presented means ± SD from three independent tests. As a key component of non-collagenous bone matrices, the main function of BGP is to maintain a normal bone mineralization rate and promote normal calcification during bone tissue mineral deposition. BMP-2 and ALP are specific indicators of osteoblasts.

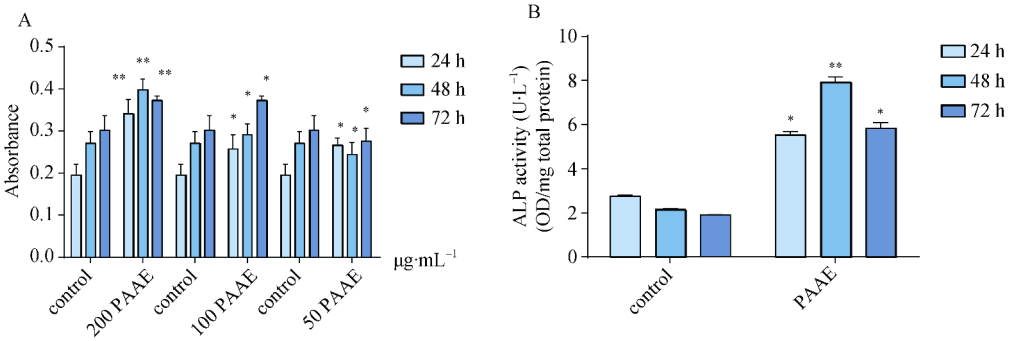

Fig. 4 The effect of pilose antler aqueous extract (PAAE) on BMSC cell proliferation and ALP activity. (A) PAAE was added to the BMSCs to final concentrations of 200, 100, and 50 μg·mL^{-1}, and the resulting mixtures were incubated for 24, 48, and 72 h. After incubation, BMSC viability was determined using the MTT analysis. (B) After different periods of incubation with PAAEs, ALP activity was evaluated using an ALP assay kit. These results suggest that PAAE treatment stimulates BMSC differentiation. Data are shown as means ± SD from three independent tests. $^{*}P < 0.05$, $^{**}P < 0.01$ *vs* control group

Bone trabeculae of the model group (Fig. 5D) became thinner and were prone to fracture, the gap between bone trabeculae increased, while the trabecular area decreased. We also found that the number of hematopoietic red blood cells decreased, and the fat vacuoles increased—two characteristic changes of osteoporosis—indicating that the model was successful. After 12 weeks of continuous administration, the trabecular arrangement of the bone was neatly arranged and could be connected to the net. The bone trabecular space was slightly enlarged in some regions and the number of hematopoietic cells in the intramedullary cavity increased. These results show that progynov, XLGB, and both the low dose and high dose PAAE treatments helped to reduce bone loss (Fig. 5D).

Finally, OVX resulted in enhanced levels of serum estrogen (E2), ALP, OCN, and BMP-2. However, treatment with PAAE resulted in a significant reduction in serum TRAP, and PPARγ-2 (Fig. 5B) compared to the OVX group. Taken together, these results indicate that the antler functions in two ways: promoting bone reconstruction and inhibiting bone absorption, thereby treating osteoporosis from two-way mode of action. In addition, the activity of BALP and the levels of BMP-2, Smad1, Smad5, Runx2, and transforming growth factor-β1 (TGF-β1) in the bone tissue were significantly enhanced (Fig. 5C) after treated with PAAE. Finally, H&E staining results reflected the protective effects of PAAE on bone loss caused by ovariectomy (Fig. 5D).

Effect of PAAE on the transcript and protein levels of Bmp-2, Smad1, Smad5, and Runx2 in rats

We used quantitative PCR to investigate the effects of PAAEs treatment on the expression of COL-1, ALP, OCN, BMP-2 and Runx2 mRNA in the bone tissues. We observed that, compared to the control group, PAAEs treatment groups showed higher transcript levels of COL-1, ALP, OCN, BMP-2, and Runx2 (Figs. 6A–6E). Western blot analyses further confirmed that higher levels of BMp-2, Runx2, Smad1, and Smad5 protein were present in PAAE-treated tissues. As shown in Figs. 6F–6I, PAAE treatment was associated with the upregulation of BMp-2, Runx2, Smad1, and Smad5 protein expression compared with the control group ($P < 0.05$).

Taken together, these results indicate that the protein levels of BMP-2 and Runx2 were enhanced by PAAE (Figs. 6G and 6I). PAAE was found to increase the phosphorylation levels of Smad1 and Smad5, whereas its effect on the expression of these two proteins was negligible (Fig. 6H). Therefore, these results suggest that PAAE stimulates the differentiation of BMSCs towards osteoblasts *via* BMP-2 signaling.

Identification and characterization of the PAAEs

PAAE has a maximum absorption (0.3478) at 298 nm (Fig. 7A). FT-IR spectrograms of PAAE shows characteristic absorption peaks of general polypeptides: the broad peak around 3400 cm^{-1} is caused by the stretching vibrations of intermolecular O-H bonds, and this signal is strong, indicating the existence of many hydrogen bonds. The acylamino group C=O is caused by the stretching vibration, suggesting that there may be -COOH bond in PAAE, and the absorption peak at 2916.59 cm^{-1} is caused by the stretching vibration of the C-H bond in structure of uronic acid. The absorption peak at 1425.77 cm^{-1} is caused by the angular vibration of the C-H bond, and the absorption peak at 900 cm^{-1} is caused by an out-of-plane deformation vibration of the -OH bond (Fig. 7B).

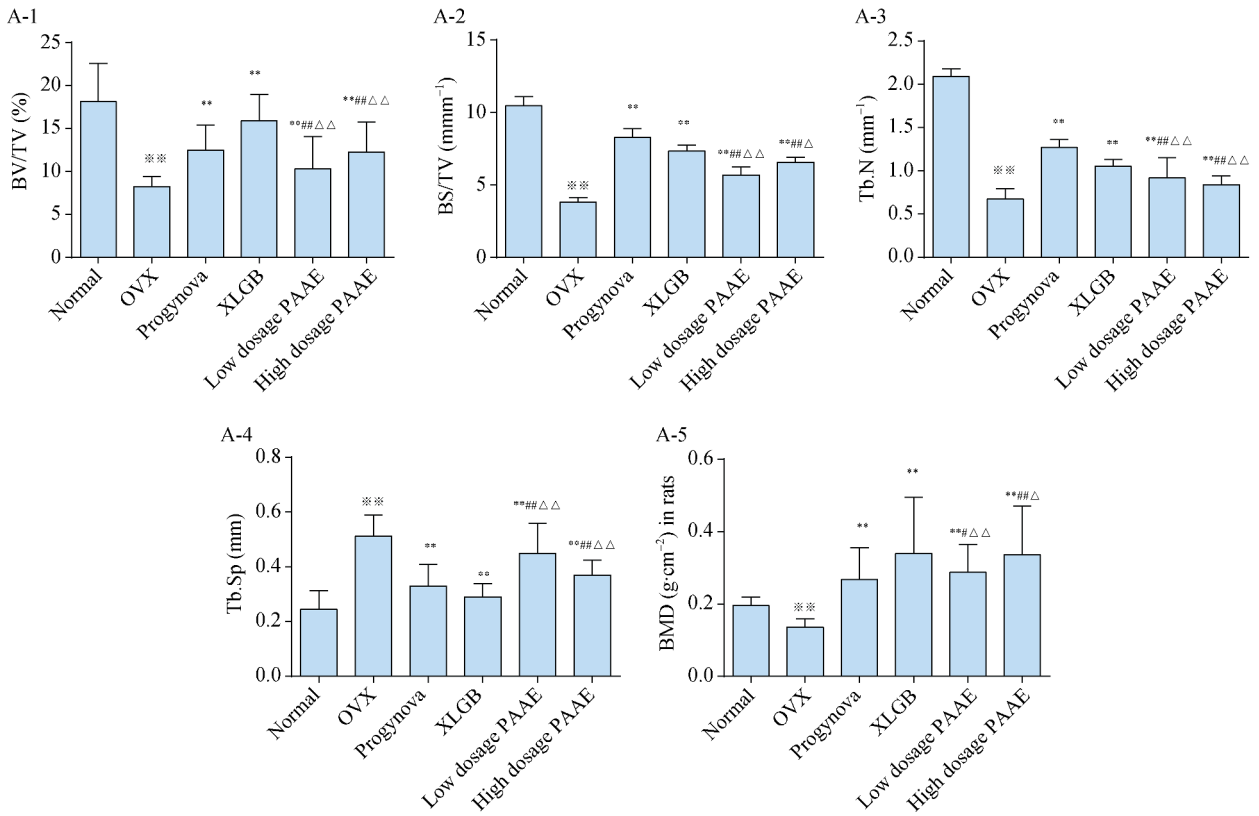

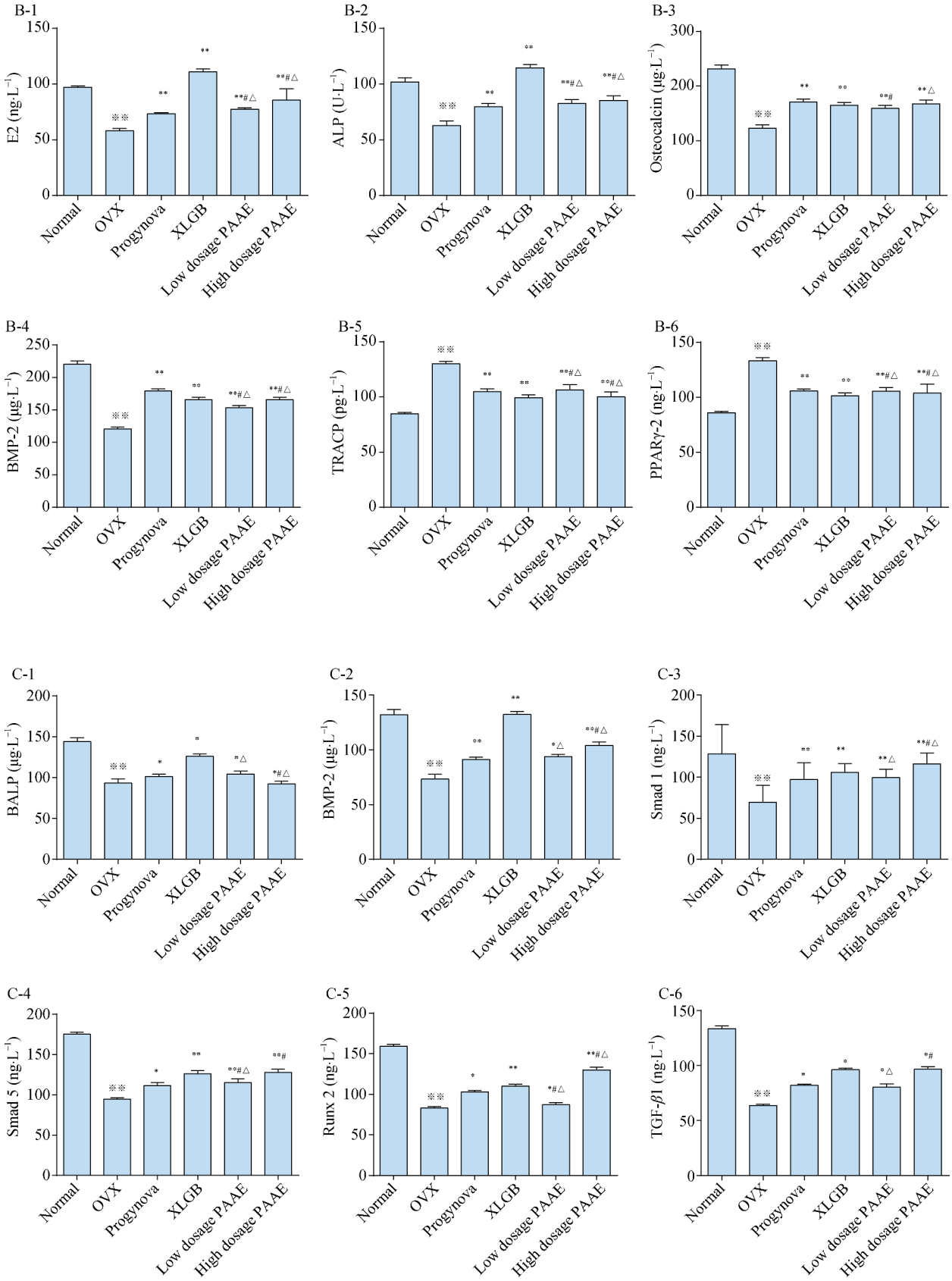
B-1
E2 (ng·L⁻¹)
B-2
ALP (U·L⁻¹)
B-3
Osteocalcin (μg·L⁻¹)
B-4
BMP-2 (μg·L⁻¹)
B-5
TRACP (pg·L⁻¹)
B-6
PPARγ-2 (ng·L⁻¹)
C-1
BALP (μg·L⁻¹)
C-2
BMP-2 (μg·L⁻¹)
C-3
Smad 1 (ng·L⁻¹)
C-4
Smad 5 (ng·L⁻¹)
C-5
Runx 2 (ng·L⁻¹)
C-6
TGF-β1 (ng·L⁻¹)
Normal
OVX
Progynova
XLGB
Low dosage PAAE
High dosage PAAE

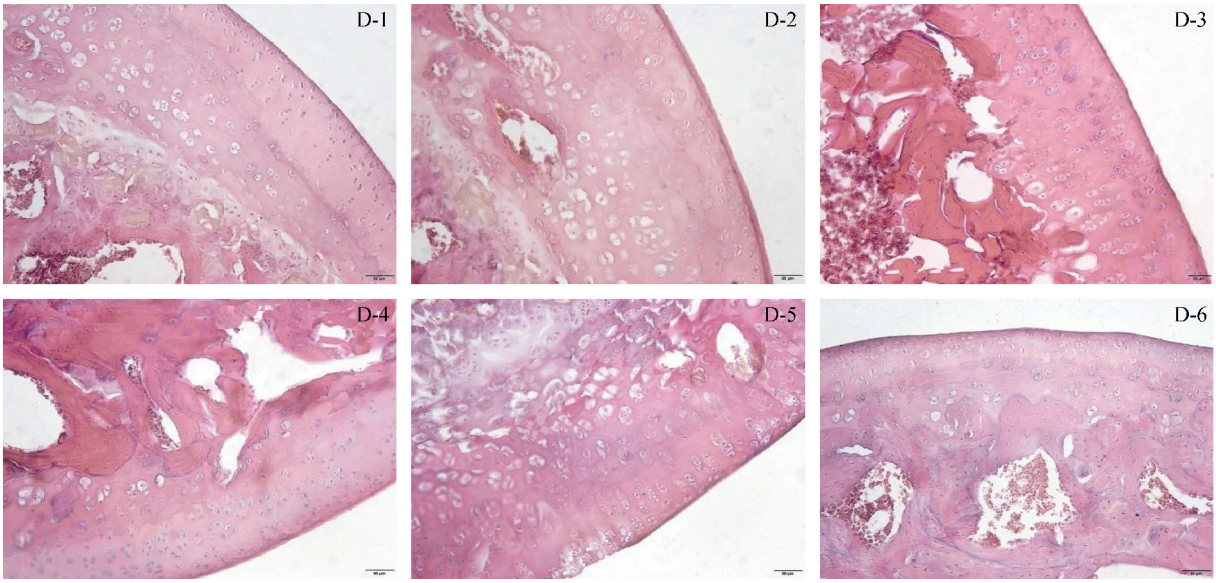

Fig. 5 Pilose antler aqueous extract (PAAE) attenuates bone loss caused by ovariectomy. (A) Microstructural parameters were analyzed based on the μCT results. Five parameters, including BV/TV, BS/TV, Tb.N, Tb.Sp, and BMD, were quantified. (B) The levels of E2, ALP, OCN, BMP-2, TRAP, and PPARγ-2 in serum were also determined by the rat ELISA kits.(C) Levels of bone alkaline phosphatase (BALP), BMP-2, Smad1, Smad5, Runx2, and transforming growth factor-β1 (TGF-β1) in the bone tissue were determined by the corresponding kits. (D) H&E staining analysis of proximal femurs (magnified 10X). Fig. D1 to Fig. D6 represent the normal group, the OVX group, the Progynova group, the XLGB group, the high dosage PAAE group, and the low dosage PAAE, respectively. Data are presented as means ± SD (n = 8–10). $^{※}P < 0.05$, $^{※※}P < 0.01$ *vs* normal group; $^{*}P < 0.05$, $^{**}P < 0.01$ *vs* OVX group; $^{\#}P < 0.05$, $^{\#\#}P < 0.01$ *vs* Progynova group; $^{\triangle}P < 0.05$, $^{\triangle\triangle}P < 0.01$ *vs* XLGB group

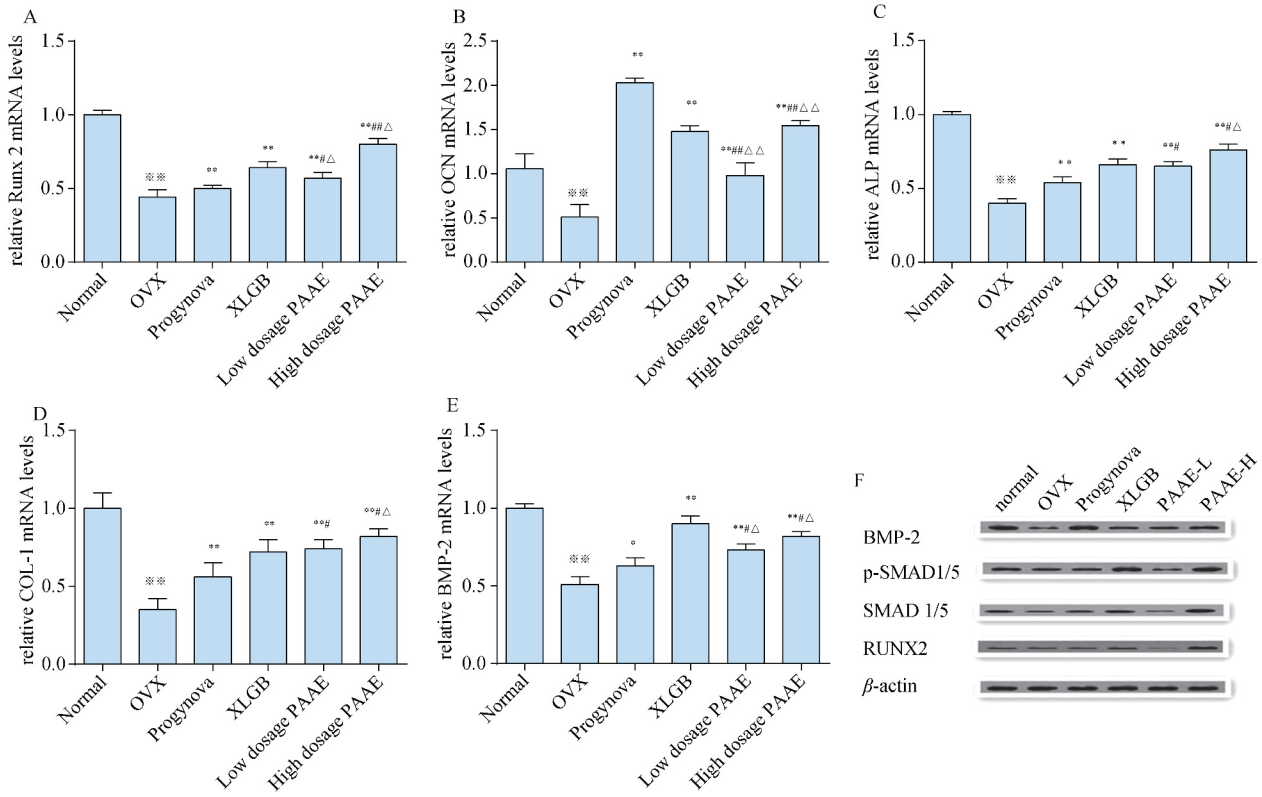

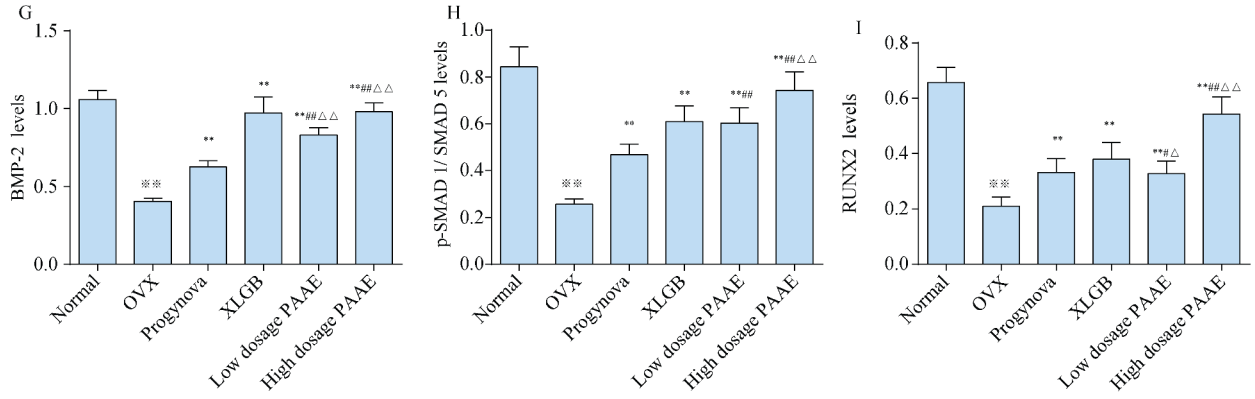

Fig. 6 Pilose antler aqueous extract (PAAE) stimulates the differentiation of BMSCs towards osteoblasts *via* BMP-2 signaling. (A–E) Relative transcript levels of *COL-I*, *OCN*, *ALP*, *BMP-2* and *Runx2* genes as revealed by qRT-PCR. (F–I) Protein levels of BMP-2, p-Smad1/5, and Runx2 after a 48 h incubation with PAAE. Densitometric assays were performed to quantify the blots. Data are presented as means ± SD from three independent tests. $^{※}P < 0.05$, $^{※※}P < 0.01$ *vs* normal group; $^{*}P < 0.05$, $^{**}P < 0.01$ *vs* OVX group; $^{\#}P < 0.05$, $^{\#\#}P < 0.01$ *vs* Progynova group. $^{△}P < 0.05$, $^{△△}P < 0.01$ *vs* XLGB group

Our MALDI-TOF MS results showed that PAAE, an aqueous extract with a molecular weight under 3000 Da, contained peaks with molecular weights of 1465.667 03, 1485.763 27, 1864.059 44, 1865.063 24, 1866.066 76, 1 867.069 72, and 1868.072 87 Da, respectively (Figs. 7C-1, 7C-2). Atomic force microscopy analysis results showed that PAAE exhibits small irregular granules. Roughness results is as follows: Rq = 0.350, and Ra = 0.199. The two-dimensional (Fig. 7D) and three-dimensional phase diagrams (Fig. 7E) are shown below. The two-dimensional phase diagram measured by AFM showed a vertical view of the surface morphology of PAAE. The three-dimensional phase diagram measured by AFM showed a side view of the surface morphology of PAAE. From the Fig. 7E, we know that the surface of PAAE is uneven, showing a three-dimensional cone-like structure.We infered that it may be because PAAE contains branched chain structure and straight chain structure. It is also because of this special undulating structure that PAAE is more easily adsorbed on the surface of cells, more easily absorbed by the human body, and plays a role in preventing and treating osteoporosis.

Discussion

Selection of dosage, action time and molecular weight of pilose antler aqueous extract (A–E)

Our results showed that aqueous extracts (A–E) of pilose antler increased the proliferation of mesenchymal stem cells and promoted bone differentiation of BMSCs. Among the aqueous extracts, PAAE A had the strongest effect and this effect maximize at a concentration of 200 μg·mL^{-1}. We also found that after 48 h, the effect of PAAE increased significantly.

Generally, in a certain concentration range, the cell experiment *in vitro* has a concentration dependence, that is, with the increase of concentration, the effect is enhanced. As for the effect of molecular weight on cell proliferation, if the molecular weight of substance is smaller, the easier it is to enter the cell, interact with the cell, and play a therapeutic role in the body. The analysis of PAAE surface morphology by atomic force microscopy (Figs. 7D–7E) shows a three-dimensional cone-like structure. It shows that the more uneven the surface morphology is, the easier it will contact cells when it enters the cell, the larger the contact area is, and the easier it will be adsorbed on the cell surface, so it will interact with cells easily.

Therefore, we chose 200 μg·ml^{-1} for 48 hours to screen which pilose antler aqueous extracts (PAAEs A–E) exerted the most significant effect on the proliferation and osteogenic differentiation of BMSCs cells. Therefore, we also chose 200 μg·mL^{-1} to complete the experiment of RNA and Western blotting. Our RNA and Western blotting experiments confirmed that PAAE A had the strongest up-regulation effect on the bmp-2/smad1 and smad5/Runx2 signal transduction pathways, which further verified the necessity of selecting PAAE A for the subsequent *in vivo* animal experiments.

Several factors related to bone formation and differentiation

Bone formation includes many steps, such as the differentiation of BMSCs into osteoblasts and the maturation and mineralization of the extracellular matrix [8]. Maturation and mineralization of the extracellular matrix are characterized by the expression of markers induced by the deposition of calcium [9]. Finally, stromal cells can undergo osteogenic differentiation into mature osteoblasts upon induction [10].

In this study, we investigated the effect of PAAE—a polypeptide-containing extract with significant pharmacological activity isolated from Cornu Cervi Pantotrichum—on BMSC differentiation and bone loss in ovariectomized rats. PAAE treatment resulted in a higher BMSC proliferation rate than in the control cells and this effect was dose-dependent. The process of osteogenic differentiation is complicated and can result in extracellular matrix mineralization. Many regulators of osteogenic differentiation are involved in this process, including ALP, BMP-2, TGF-β, Runx2, OCN (BGP), etc.

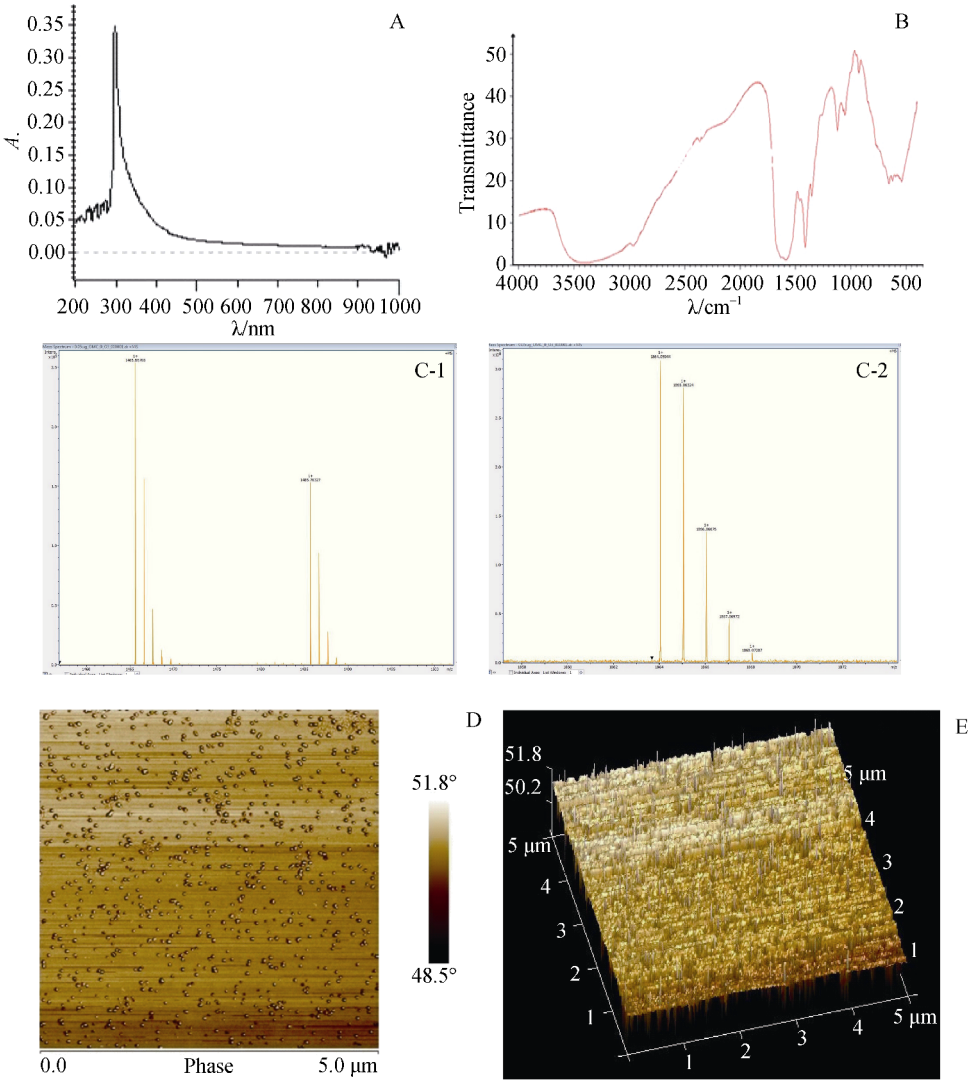

Fig. 7 Identification and characterization of pilose antler aqueous extract (PAAE). (A) Ultraviolet-visible absorption spectrum of PAAE. (B) Infrared absorption spectrum of PAAE. (C-1 , C-2) Peptide spectrum of PAAE by MALDI-TOF MS analysis. (D) Two-dimensional phase diagram of PAAE by AFM. (E) Three-dimensional phase diagram of PAAE by AFM

ALP and BGP are specific markers involved in the early and middle processes of differentiation [11]. BMP-2 is one of the most important extracellular signaling molecules that promote bone formation and osteoblast differentiation. It plays a role in osteogenesis by activating SmadS signaling and regulating the transcription of osteogenic related genes. The Smads (Smads 1–9) are BMP signaling proteins, Smad2 and Smad3 can transfer TGF-β activin signal, and Smad1, Smad5, Smad8, and Smad9 regulate BMP signal transduction. Runx is a group of specific transcription factor that regulates osteogenic differentiation, and this family includes Runx1, Runx2, and Runx3. Runx2 is a target of BMP-2. Runx2 is an important regulator of BMSC and osteoblast (OB) differentiation and bone development and plays a crucial role in osteoblast differentiation. After BMP-2 activates Smad1, Smad5, and Smad8, the expression of Runx2 is activated by both a distal P1 promoter and a proximal P2 promoter, and the level of functional Runx2 determines the degree of bone maturation and conversion.

TRAP is an enzyme closely related to the degradation of bone matrix secreted by osteoclasts. The level of TRAP inserum indicates the degree of bone resorption [5]. Previous studies have shown that PPARγ-2 is crucial for regulating the conversion between osteoblasts and osteoclasts that determines bone mass. Moreover, this process is closely related to osteoporosis. BMSCs are known to be affected by PPARγ-2 during their differentiation towards adipocyte [12-13]. That is, when the proportions of adipocytes and osteoblasts in the marrow cavity are imbalanced, the morphological structure of the bone changes, leading to osteoporosis [14-15]. TGF-β is the most abundant bone growth factor that can regulate osteoblast proliferation and differentiation, as well as stimulate collagen and bone matrix protein synthesis. It is a potential regulator of bone induction and also known to regulate osteogenic differ-

entiation [16-18].

Conclusions

PAAE could promote the proliferation and differentiation of BMSCs. PAAE exerted the maximize effect on BMSCs at a concentration of 200 μg·mL^{-1}, significantly at 48 h. Moreover, the trabecular microarchitecture of ovariectomized rats was also found to be protected by PAAE in a dose-dependent manner. PAAE activated the BMP-2/Smad1, 5/Runx2 pathway to induce osteoblastic differentiation and mineralization in the BMSCs and could inhibit OVX-induced bone loss. These mechanisms are likely responsible for the therapeutic effect of PAAE on postmenopausal osteoporosis.

References

[1] Baccaro LF, Conde DM, Costa-PaivaL, *et al*. The epidemiology and management of postmenopausal osteoporosis: a viewpoint from Brazil [J]. *Clin Interv Aging*, 2015, **10**: 583-591.

[2] Diab DL, Watts NB. Postmenopausal osteoporosis [J]. *Curr Opin Endocrinol Diabetes Obes*, 2013, **20**(6): 501-509.

[3] Isenbarger DW, Chapin BL. Osteoporosis. Current pharmacologic options for prevention and treatment [J]. *Postgrad Med*, 1997, **101**(1): 129-132, 136-137, 141-142.

[4] *Pharmacopoeia of the People's Republic of China* [S]. (Part I). 2015: 323-324

[5] Gong W. *Study on the Relationship between the Role of "Tonifying the Kidney and Strengthening Bone" and the Quality of the Pilose Antler* [D]. Shenyang: Liaoning University of Traditional Chinese Medicine, 2011.

[6] Gong W, Li F. Cervi cornu pantotrichun aqueous extract promote osteoblasts differentia-tion and bone formation [J]. *Biomed Res*, 2014, **25**(2): 249-252.

[7] Cornu cervi pantotrichum [EB/OL]. https: //baike.so.com/doc/1713898-1811958.html 2009.

[8] Komori T. Regulation of bone development and maintenance by Runx2 [J]. *Front Biosci*, 2008, **13**: 898-903.

[9] Gaur T, Hussain S, Mudhasani R, *et al*. Dicer inactivation in osteoprogenitor cells compromises fetal survival and bone formation, while excision in differentiated osteoblasts increases bone mass in the adult mouse [J]. *Dev Biol*, 2010, **340**(1): 10-21.

[10] Koruna M, Kato J, Chiba H, *et al*. Telomerized human bone marrow-derived cell clones maintain the phenotype of hematopoietic-supporting osteoblastic and myofibroblastic stromal cells after long-term culture [J]. *Exp Hematol*, 2005, **33**(12): 1544-1553.

[11] Hu ZM, Peel SA, SK HO, *et al*. Induction of bone matrix protein expression by native bone matrix proteins in C2C12 culture [J]. *Biomed Environ Sci*, 2009, **22**(2): 164-169.

[12] Li CQ, He LC, Dong HY, *et al*. Screening for the anti-inflammatory activity of fractions and compounds from Atractylodes macrocephala koidz [J]. *J Ethnopharmacol*, 2007, **114**(2): 212-217.

[13] Lee JC, Lee KY, Son YO, *et al*. Stimulating effects on mouse spleuocytes of glycoproteins from the herbal medicine Atractylodes macrocephala Koidz [J]. *Phytomedicine*, 2007, **14**(6): 390-395.

[14] Shi CD, Yang YH, Yu X, *et al*. Effect of KangshuJiangu Granules on the expression of PPARγ-2 of bone tissue from ovariectomized osteoporosis model rats [J]. *J Sichuan Tradit Chin Med*, 2015, **33**(2): 61-64.

[15] Hu J, Zhang AB, Liu XL, *et al*. Extracorporeal shock wave promotes differentiation of human bone marrow stromal cells into osteoprogenitors [J]. *Chin J Exp Surg*, 2005, **22**(2): 147-150.

[16] Sun WP, Li FS, Chen C, *et al*. Immunomodulation of Atractylodis polysaccharides in mice [J]. *Chin J Microecol*, 2011, **23**(10): 881-882, 886.

[17] Kim K, Dean D, Wallace J, *et al*. The influence of stereolithographic scaffold architecture and composition on osteogenic signal expression with rat bone marrow stromal cells [J]. *Biomaterials*, 2011, **32**(15): 3750-3763.

[18] Ren YL, Li YL, Lv HB, *et al*. Expressions of TGF-β1/Smad4 mRNA of kidney by Zuogui Pill in ovariectomy-induced osteoporosis rats [J]. *Chin J Exp Tradit Med Form*, 2012, **18**(10): 190-194.

Cite this article as: REN Cong, GONG Wei , LI Feng, XIE Ming. Pilose antler aqueous extract promotes the proliferation and osteogenic differentiation of bone marrow mesenchymal stem cells by stimulating the BMP-2/Smad1, 5/Runx2 signaling pathway [J]. *Chin J Nat Med*, 2019, **17**(10): 756-767.